PROCEEDINGS OF ECOS 2023 - THE 36TH INTERNATIONAL CONFERENCE ON
EFFICIENCY, COST, OPTIMIZATION, SIMULATION AND ENVIRONMENTAL IMPACT OF ENERGY SYSTEMS
25-30 JUNE 2023, LAS PALMAS DE GRAN CANARIA, SPAIN

Exergoeconomic analysis of a system for liquefaction and purification of captured CO_2

Rikke C. Pedersen [a], Torben Ommen [b], Erasmus Rothuizen [c], Brian Elmegaard [d] and Jonas K. Jensen [e]

[a] Technical University of Denmark, Dept. of Civil & Mechanical Engineering, Kgs. Lyngby, DK, rikpe@dtu.dk, CA
[b] Sensible Energy A/S, Ballerup, DK, tso@sensibleenergy.dk
[c] Sensible Energy A/S, Ballerup, DK, edr@sensibleenergy.dk
[d] Technical University of Denmark, Dept. of Civil & Mechanical Engineering, Kgs. Lyngby, DK, brel@dtu.dk
[e] Technical University of Denmark, Dept. of Civil & Mechanical Engineering, Kgs. Lyngby, DK, jkjje@dtu.dk

Abstract:

The most severe reason for global warming is the release of anthropogenic CO_2 emissions to the atmosphere. One way to mitigate these emissions is to capture CO_2 directly at an emitting source using carbon capture technologies. An important process in the carbon capture value chain is to condition the captured CO_2 to the following transportation. In this study, a system for liquefaction and purification of CO_2 is of focus and an exergoeconomic analysis is made. In the system, CO_2 is compressed through two-stage compression with intercooling, while water condensate is removed. The liquefaction is performed using an external two-stage refrigeration cycle. The compressors were found to be the greatest source of exergy destruction and were the greatest cost contributors. An overall exergy efficiency of 39 % was found and it was seen that 13 % of the fuel supplied was lost in external coolers. To improve the system and utilise the exergy loss, two configurations for district heat integration were investigated. It was found to increase the exergy efficiency to 45 % and 50 %, respectively, depending on the configuration. Integration of district heating in the intercoolers could be made without additional costs for the system. A cost increase of the overall system of 11 % was seen when the heat discharged in the refrigeration cycle was also utilised for district heat production. This shows that there is a potential for utilising the waste heat from the system and adding revenue from district heat sales.

Keywords:

CO_2 liquefaction and purification; CO_2 conditioning; District heat integration; Exergoeconomic analysis; Thermoeconomic analysis.

1. Introduction

In 2016, anthropogenic CO_2 emissions accounted for 75 % of the total greenhouse gas emissions in the world [1]. Some of the sectors responsible for the majority of the CO_2 emissions are the electricity and heating sector and the manufacturing and construction sector accounting for 41 % and 17 %, respectively. Carbon capture technologies are expected to play an important role in reducing emissions from these sectors, as the technology allows for continuous utilisation of existing fossil-based facilities and can provide deep emission reductions that are difficult to mitigate with technological advances (e.g. for production of iron, steel, cement, and various chemicals) [2]. Furthermore, the technology can be used to achieve negative emissions by capturing and storing CO_2 from biogenic sources. A capture capacity of 7.6 Gt CO_2 per year is expected in 2050 [3], of which only 0.5 % was realised in 2021 [4]. This indicates that all process steps of the carbon capture value chain must be scaled up and become more cost-effective to reach the required capacity. The focus of this study is the liquefaction and purification process, which ensures that captured CO_2 is conditioned to the correct state and quality before transport. The process is highlighted in the carbon capture value chain in Fig. 1. The conditioning process accounts for between 20 % and 70 % of the costs when also considering the following transportation [5, 6, 7]. Therefore, an improvement of this process step can potentially have a significant influence on the overall costs.

The captured CO_2 is typically in a gaseous state after separation. To reduce the cost of transportation, the density can be increased. This can be achieved in the conditioning process by increasing the pressure or decreasing the temperature of CO_2. In the food and beverage industry today, CO_2 is transported in a liquid state at 15 bar and –30 °C [8]. Furthermore, impurities such as water, volatiles, and incondensable gasses could be removed before transportation [9].

Several studies have compared different layouts of the liquefaction and purification system on energy [10, 11]

https://doi.org/10.52202/069564-0015

Figure 1: Position of the liquefaction and purification process in the carbon capture value chain.

and economic [12, 13] performance parameters when different requirements for the end-state of CO_2 exist. At a delivery pressure of 15 bar, a system with an external refrigeration cycle generally shows the best performance. The effects of impurities and final quality requirement are investigated by Deng et al. [8], they find that the process costs increase when impurities in the source increase at lower delivery pressures. Aspelund and Jordal [9] investigate the effects of impurities and pressure level of the CO_2 feed gas. They find that a decrease in the inlet pressure and an increase in impurities increase power consumption. Energy, exergy, and economic analyses have been performed on different layouts of a CO_2 liquefaction system by Chen and Morosuk [14], showing that the majority of the exergy destruction ($>$80 %) occurs in coolers and compressors and that it is equally distributed between these two types of components. The highest exergy efficiency of 67 % was found for a system with an external refrigeration cycle. An exergoeconomic analysis was made on a liquefaction system using an absorption refrigeration cycle by Aliyon et al. [15] having an exergy efficiency of 86 % with heat exchangers showing the highest cost improvement potential. Exergy analyses have also been performed on liquefaction systems by Muhammad et al. [16, 17] resulting in total exergy efficiencies of 68 % and 56 %, respectively. It is seen that the highest exergy destruction occurs during compression of the captured CO_2 and that potential for utilisation of heat from intercooling exists. It is of interest to determine where cost inefficiencies exist in a liquefaction system using an external refrigeration cycle to deliver purified liquid CO_2 at 15 bar, and whether it is possible to recover heat through the integration of district heat (DH) production. Therefore, an exergoeconomic analysis of a liquefaction and purification system was made in the present study. It was investigated which components were of most importance for the overall costs of the system and whether thermodynamic inefficiencies or capital expenses were dominating sources of costs. The potential of DH integration was evaluated to determine the economic benefit for the system.

2. Methods

2.1. System description

A process flow diagram of the baseline liquefaction and purification system is illustrated in Fig. 2. The CO_2 product stream is compressed through two-stage compression (COMP) with intercooling (COOL). During intercooling, the remains of water in the captured CO_2 are condensed and removed in gas-liquid separators (SEP). The compressed and purified CO_2 is then liquefied in a heat exchanger (LIQHEX) which works as the evaporator of an external transcritical CO_2 refrigeration cycle. Finally, the liquid CO_2 is pumped to the transport pressure. The incoming mass flow rate of 1.8 th^{-1} of gaseous CO_2 was at 40 °C and 1.7 bar containing 4.3 %(mol) water. Remaining impurities were neglected. The system should deliver liquid CO_2 at 15 bar and 2 K subcooling, and the liquefaction was set to occur at 14.5 bar. In the baseline system, cooling water was heated from 20 °C to 70 °C in the intercoolers, while air was heated from 15 °C to 40 °C in the gascooler (GC). DH was integrated in two alternative ways; in all intercoolers and the gascooler (COOL1, COOL2, COOL3, and GC), and only in intercoolers (COOL1, COOL2, and COOL3). DH water was assumed to be heated from 35 °C to 70 °C. The high pressure in the refrigeration cycle was optimised to the temperature of the available cooling media through cost minimisation. The optimal pressure with air as cooling media in the GC was 75 bar, while the optimal pressure was 110 bar when DH was integrated in the GC. In two-stage compression, the same pressure ratio was applied for each stage, and the intermediate pressure levels (p_{int}) were given by: $p_{int} = \sqrt{p_{low} \cdot p_{high}}$ [18].

2.2. Energy analysis

The system was modelled in steady state by applying mass and energy balances to control volumes for all components. Pressure and heat losses were neglected in pipelines, heat exchangers, and separators. The model was implemented in Engineering Equation Solver [19], and the thermodynamic properties of the CO_2 stream with water impurities were determined using Dalton's law and an ideal gas mixture assumption.

Reciprocating compressors were used in the system and were modelled using a heat loss factor, an isentropic efficiency (η_s), and a volumetric efficiency (η_{vol}). A heat loss factor of 3 % was applied and defined as the ratio of the compressor heat loss to the supplied compressor power. The estimated efficiencies for compressors and pump are presented in Table 1.

The heat exchangers were modelled with a minimum temperature approach of 5 K[1] and a constant overall heat transfer coefficient (U), as shown in Table 2.

https://doi.org/10.52202/069564-0015

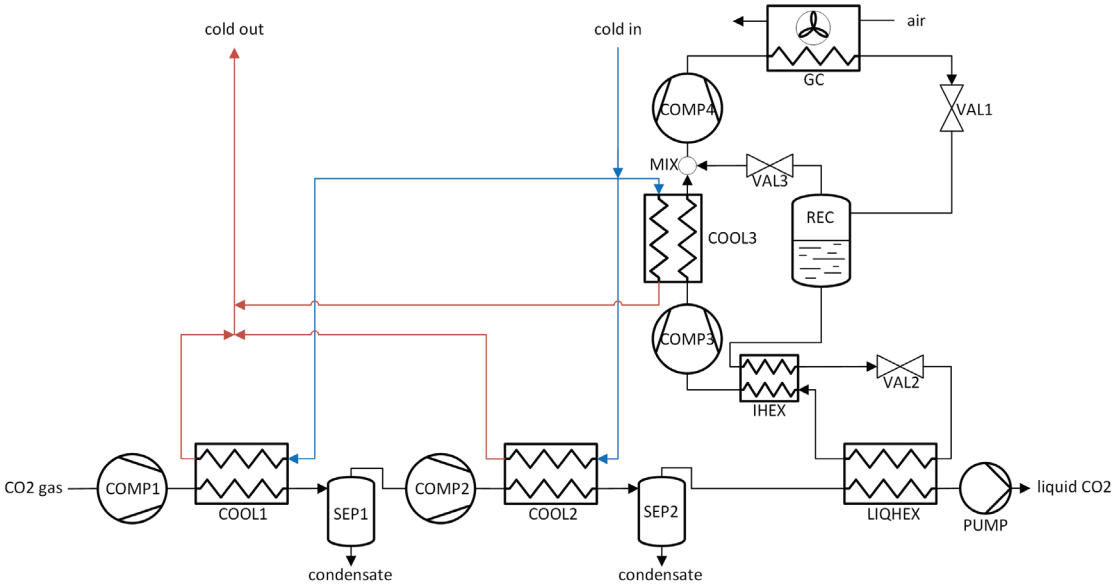

Figure 2: Process flow diagram of the baseline liquefaction and purification system.

Table 1: Assumed efficiencies. Component names refer to Fig. 2.

Component	η_s [%]	η_{vol} [%]
COMP1, COMP2	65	80
COMP3, COMP4	67	83
PUMP	85	100

The gas-liquid separators were assumed to collect all liquid from the two-phase mixture at the bottom of the tank by gravitational forces. The vertical velocity (v) was assumed to be 0.30 ms^{-1} for SEP1, 0.05 ms^{-1} for SEP2 and, 0.13 ms^{-1} for the receiver in the refrigeration cycle (REC). SEP2 in the CO_2 product stream was assumed to remove all remains of water so that pure CO_2 entered the liquefaction heat exchanger.

The required size of each component was determined using the relations given in Table 3. The compressors and pump were defined by a displacement volume ($\dot{V}_{disp}$) required to deliver the actual volume flow rate at the suction line ($\dot{V}_{in}$). The required heat transfer area (A) of the heat exchangers were determined from the required heat transfer rate ($\dot{Q}$), the overall heat transfer coefficient and the logarithmic mean temperature difference of the process (ΔT). The gas-liquid separators had a cross-sectional area (A_{cross}) which ensured the assumed vertical velocity of the volume flow of gas ($\dot{V}_{gas,out}$).

Table 2: Assumed overall heat transfer coefficients. Component names refer to Fig. 2.

Component	U [kW(m^{2}K)$^{-1}$]	Source
LIQHEX	1.20	[20]
IHEX	0.46	[20]
COOL1	0.46	*NDA*
COOL2, COOL3	0.68	*NDA*
GC (air as cooling media)	0.04	[21]
GC (DH water as cooling media)	2.30	*NDA*

2.3. Exergy analysis

The exergy of a given system is the useful work that can potentially be utilised in a process where the system interacts and reaches equilibrium with the surroundings, while heat transfer only occurs to the surroundings [22].

[1] To allow the model to reach the optimal pressure of 110 bar when DH was integrated in the GC, the pinch point temperature difference in the internal heat exchanger (IHEX) was increased from 5 K to 8 K.

Table 3: Relations for calculation of required component sizes.

Component type	Size relation
Compressors and pump	$\dot{V}_{\text{disp}} = \dot{V}_{\text{in}}/\eta_{\text{vol}}$
Heat exchangers	$A = \dot{Q}/U\Delta T$
Gas-liquid separators	$A_{\text{cross}} = \dot{V}_{\text{gas,out}}/v$

An exergy analysis helps identify which components and material streams are the cause of inefficiencies and losses in the system. The surroundings (denoted state 0) were defined with a temperature and pressure of 15 °C and 1 atm. An exergy reference environment was chosen and the standard chemical exergy (e_0^{CH}) of CO_2 and H_2O was given as 19 870 kJ/kmol and 9500 kJ/kmol, respectively [22]. The specific exergy (e) was calculated by Eq. (1) [22] taking the physical (PH) and chemical (CH) exergy into account. This was used together with the mass flow rate ($\dot{m}$) to determine the exergy flow rates ($\dot{E}$) through the system: $\dot{E} = e \cdot \dot{m}$.

$$e = \underbrace{(h - h_0) - T_0\,(s - s_0)}_{e^{\text{PH}}} + \underbrace{\sum_n \left(y_n e_{0,n}^{\text{CH}}\right) + \left(h_0 - \sum_n y_n h_{n,0}\right) - T_0 \left(s_0 - \sum_n y_n s_{n,0}\right)}_{e^{\text{CH}}} \tag{1}$$

The exergy destruction within the system was determined using the product (P) and fuel (F) concepts [23]. The rate of fuel exergy should be sufficient to generate the product and overcome the exergy destruction (D) and exergy losses (L), as given by Eq. (2) [22]. Losses were considered as material streams which transfer exergy directly to the surroundings without further use and were only considered on a system level. Therefore, the last term of Eq. (2) was omitted on a component level.

$$\dot{E}_{\text{F}} = \dot{E}_{\text{P}} + \dot{E}_{\text{D}} + \dot{E}_{\text{L}} \tag{2}$$

The definitions of product and fuel exergy flow rates are given in Table 4. The external coolers, mixer and valves were considered to be dissipative components, therefore no product was defined. The overall product of the baseline system was the increase in exergy of the CO_2 product stream, while the exergy fuel accounted electricity consumption and cooling water (denoted COOL). When DH was integrated in the system, the heating of the cooling water was also considered as a product and the fuel reduced to only being the electricity consumption. For the baseline system, the overall losses were given as the sum of the condensate of water leaving the separators, all leaving streams of cooling water, and the air stream leaving the GC, as given by Eq. (3).

$$\dot{E}_{\text{L}} = \sum \left(\dot{E}_{\text{liq,out}} + \dot{E}_{\text{COOL,out}}\right) + \dot{E}_{\text{GC,out}} \tag{3}$$

Table 4: Definitions of fuel and product exergy rates. Component names refer to Fig. 2.

Component type	$\dot{E}_{\text{F}}$	$\dot{E}_{\text{P}}$
COMP	$\dot{W}$	$\dot{E}_{\text{out}} - \dot{E}_{\text{in}}$
PUMP	$\dot{W}$	$\dot{E}_{\text{out}} - \dot{E}_{\text{in}}$
SEP	$\dot{E}_{\text{in}} - \dot{E}_{\text{liq,out}}$	$\dot{E}_{\text{gas,out}}$
REC	$\dot{E}_{\text{in}}$	$\dot{E}_{\text{gas,out}} + \dot{E}_{\text{liq,out}}$
LIQHEX (cooling across T_0)	$(\dot{E}_{\text{ref,in}} - \dot{E}_{\text{ref,out}}) + \dot{E}_{\text{CO2,in}}$	$\dot{E}_{\text{CO2,out}}$
IHEX (cooling at $T < T_0$)	$\dot{E}_{\text{cold,in}} - \dot{E}_{\text{cold,out}}$	$\dot{E}_{\text{hot,out}} - \dot{E}_{\text{hot,in}}$
COOL (cooling at $T > T_0$)	$\left(\dot{E}_{\text{CO2,in}} - \dot{E}_{\text{CO2,out}}\right) - \left(\dot{E}_{\text{COOL,out}} - \dot{E}_{\text{COOL,in}}\right)$	–
GC (cooling at $T > T_0$)	$\left(\dot{E}_{\text{ref,in}} - \dot{E}_{\text{ref,out}}\right) + \dot{W} - \dot{E}_{\text{a,out}}$	–
MIX	$\dot{E}_{\text{hot,in}} + \dot{E}_{\text{cold,in}} - \dot{E}_{\text{out}}$	–
VAL	$\dot{E}_{\text{in}} - \dot{E}_{\text{out}}$	–
Baseline system	$\sum \left(\dot{W} + \dot{E}_{\text{COOL,in}}\right)$	$\dot{E}_{\text{CO2,out}} - \dot{E}_{\text{CO2,in}}$
DH integration	$\sum \dot{W}$	$\left(\dot{E}_{\text{CO2,out}} - \dot{E}_{\text{CO2,in}}\right) + \sum \left(\dot{E}_{\text{COOL,out}} - \dot{E}_{\text{COOL,in}}\right)$

https://doi.org/10.52202/069564-0015

For the system with DH integration in the intercoolers, the losses reduced to only account the condensate of water leaving the separators and the air stream leaving the GC, as given by Eq. (4).

$$\dot{E}_{\mathrm{L}} = \sum \dot{E}_{\mathrm{liq,out}} + \dot{E}_{\mathrm{GC,out}} \tag{4}$$

When DH was integrated in all external coolers, the losses only included the condensate of water leaving the separators, as given by Eq. (5).

$$\dot{E}_{\mathrm{L}} = \sum \dot{E}_{\mathrm{liq,out}} \tag{5}$$

A set of exergy performance indicators can be defined to evaluate individual components and the system as a whole. An exergy destruction ratio (γ_{D}) was defined for each component and on a system level, see Eq. (6) [22]. An exergy loss ratio (γ_{L}) was similarly defined for each material stream considered as a loss and on a system level as seen in Eq. (7). An exergy efficiency (ε) was defined for all non-dissipative components and on a system level and was given as the ratio of the exergy product rate to the exergy fuel rate: $\varepsilon = \dot{E}_{\mathrm{P}}/\dot{E}_{\mathrm{F}}$. For the dissipative components, no exergy efficiency was defined.

$$\text{component level}: \quad \gamma_{\mathrm{D}} = \frac{\dot{E}_{\mathrm{D}}}{\dot{E}_{\mathrm{D,sys}}}, \qquad \text{system level}: \quad \gamma_{\mathrm{D,sys}} = \frac{\dot{E}_{\mathrm{D,sys}}}{\dot{E}_{\mathrm{F,sys}}} \tag{6}$$

$$\text{stream level}: \quad \gamma_{\mathrm{L}} = \frac{\dot{E}_{\mathrm{L}}}{\dot{E}_{\mathrm{L,sys}}}, \qquad \text{system level}: \quad \gamma_{\mathrm{L,sys}} = \frac{\dot{E}_{\mathrm{L,sys}}}{\dot{E}_{\mathrm{F,sys}}} \tag{7}$$

2.4. Economic analysis

For each component, the purchased equipment cost (PEC) was estimated by the cost relation in Eq. (8) [22]. The PEC of a component with a given size (X) was estimated using the list price of a similar component (denoted z) with a known size. The scaling exponent (α) is specific for each component type and is given in Table 5. The PEC of the reference components are presented in Table 6. All monetary values are given in 2022€.

$$\mathrm{PEC} = \mathrm{PEC}_z \left(\frac{X}{X_z}\right)^{\alpha} \tag{8}$$

Table 5: Scaling exponents used for different types of components.

Component type	**Scaling exponent** (α)	**Source**
Compressors	0.77	[24]
Pump	0.59	[25]
Heat exchangers with CO_2 or water	0.78	[25]
External cooler with air	0.39	[25]
Gas-liquid separators	0.30	[22]

To account for additional costs besides the investment of the component, the PEC was adjusted to a total capital investment of TCI = 4.16 · PEC [22]. The levelised cost rate associated with the capital investment ($\dot{Z}^{\mathrm{CI}}$) was then given by Eq. (9). Here, the TCI was discounted and annualised using a real discount rate (i) of 3 % and a lifetime (L) of 25 years. An annual operating time (H) of 8000 h was assumed. The cost rate of operation and maintenance was given by $\dot{Z}^{\mathrm{OM}} = 0.15 \cdot \dot{Z}_k^{\mathrm{CI}}$ [25]. The total costs associated with owning a component ($\dot{Z}$) was the sum of capital investment and operation and maintenance: $\dot{Z} = \dot{Z}^{\mathrm{CI}} + \dot{Z}^{\mathrm{OM}}$.

$$\dot{Z}^{\mathrm{CI}} = \frac{\mathrm{TCI}\left(\frac{i(1+i)^L}{(1+i)^L-1}\right)}{H\,3600\mathrm{sh}^{-1}} \tag{9}$$

The electricity price was assumed to be 0.08 €kWh^{-1} based on [29] and [30]. The cost of the cooling media was 7.83 €kWh^{-1} and was calculated from the TCI and operational costs of a drycooler required to discharge the heat to the surroundings. The entering gaseous CO_2 and the entering DH water were assumed to be free of charge.

Table 6: Purchased equipment cost and size of reference component for all components in the system. Component names refer to Fig. 2.

Component	PEC of reference [€]	Size of reference (X)	Source
COMP1, COMP2, COMP3	34 393	150.5 m^3h^{-1}	[26]
COMP4	66 731	112.8 m^3h^{-1}	[26]
PUMP	4956	5.7 m^3h^{-1}	[27]
LIQHEX	2426	13.5 m^2	[28]
IHEX	452	1.97 $m^{2\dagger}$	[28]
COOL1	2177	7.69 $m^{2\dagger}$	*NDA*
COOL2, COOL3	1128	6.07 $m^{2\dagger}$	*NDA*
GC (air as cooling media)	14 695	464 m^2	[21]
GC (DH water as cooling media)	2223	17.1 m^2	*NDA*
SEP1	5335	0.29 m^3	*NDA*
SEP2	6018	0.29 m^3	*NDA*
REC	1228	0.03 m^{3*}	[26]
VAL1	1926	–	[26]
VAL2, VAL3	1110	–	[26]
MIX	68	–	[26]

Range of cost function: *0.07 m^3 to 150 m^3, †8.3 m^2 to 373 m^2. It was assumed that prices were still representative.

2.5. Exergoeconomic analysis

An exergoeconomic analysis is a way to determine cost flows throughout a thermal energy system and to investigate how inefficiencies in the system affect the cost of the final product [22]. The cost rates ($\dot{C}$) were determined throughout the system, and are given as the product of the average cost per unit of exergy (c) and the exergy flow rate: $\dot{C} = c \cdot \dot{E}$ [22]. The cost balances applied to all types of components are given in Table 7. Auxiliary cost equations were made for components with more than one exiting exergy stream using the product and fuel principles according to the approach in [23]. The cost balances of dissipative components (coolers, mixer, and valves) were adjusted so that all costs were assigned to an auxiliary variable ($\dot{C}_{\mathrm{dif,dc}}$), which was added to the final product. The costs of all loss streams were set to 0 €s^{-1} in the analysis, thereby the costs were assigned directly to the overall product. On a system level, the economic value of the losses was estimated by assuming an overall constant product rate and that changes in losses result in changes in the fuel supply: $\dot{C}_{\mathrm{L}} = c_{\mathrm{F}} \cdot \dot{E}_{\mathrm{L}}$, where c_{F} is the average cost per unit of exergy fuel. A similar assumption was used for estimating the costs of exergy destruction: $\dot{C}_{\mathrm{D}} = c_{\mathrm{F}} \cdot \dot{E}_{\mathrm{D}}$ [22].

The cost balance of the general form: $\dot{C}_{\mathrm{P}} = \dot{C}_{\mathrm{F}} + \dot{Z}$ was applied on a system level with the definitions of product and fuel costs given in Table 8. For the systems with DH integration, the cost rate of the total product was given as the sum of the cost rate of CO_2 and DH production: $\dot{C}_{\mathrm{P}} = \dot{C}_{\mathrm{P,CO2}} + \sum \dot{C}_{\mathrm{P,DH}}$. The definition of product and fuel exergy used for the external coolers was the same in both the baseline system and with DH integration, as this allowed for allocation of the component costs to both DH production and the CO_2. When DH was produced

Table 7: Cost balances and auxiliary equations for each component. Component names refer to Fig. 2.

Component type	Cost balance	Auxiliary equation (*F/P principle*)
COMP	$\dot{C}_{\mathrm{out}} = \dot{C}_{\mathrm{in}} + \dot{C}_{\mathrm{w}} + \dot{Z}$	–
PUMP	$\dot{C}_{\mathrm{out}} = \dot{C}_{\mathrm{in}} + \dot{C}_{\mathrm{w}} + \dot{Z}$	–
SEP	$\dot{C}_{\mathrm{gas,out}} = \dot{C}_{\mathrm{in}} + \dot{Z}$	
REC	$\dot{C}_{\mathrm{gas,out}} + \dot{C}_{\mathrm{liq,out}} = \dot{C}_{\mathrm{in}} + \dot{Z}$	$(P)\ c_{\mathrm{gas,out}} = c_{\mathrm{liq,out}}$
LIQHEX	$\dot{C}_{\mathrm{CO2,out}} + \dot{C}_{\mathrm{ref,out}} = \dot{C}_{\mathrm{CO2,in}} + \dot{C}_{\mathrm{ref,in}} + \dot{Z}$	$(F)\ c_{\mathrm{ref,in}} = c_{\mathrm{ref,out}}$
IHEX	$\dot{C}_{\mathrm{hot,out}} + \dot{C}_{\mathrm{cold,out}} = \dot{C}_{\mathrm{cold,in}} + \dot{C}_{\mathrm{hot,in}} + \dot{Z}$	$(F)\ c_{\mathrm{cold,in}} = c_{\mathrm{cold,out}}$
COOL	$\dot{C}_{\mathrm{dif,dc}} + \dot{C}_{\mathrm{CO2,out}} = \dot{C}_{\mathrm{CO2,in}} + \dot{C}_{\mathrm{COOL,in}} + \dot{Z}$	$(F)\ c_{\mathrm{CO2,in}} = c_{\mathrm{CO2,out}}$
GC	$\dot{C}_{\mathrm{dif,dc}} + \dot{C}_{\mathrm{ref,out}} = \dot{C}_{\mathrm{ref,in}} + \dot{C}_{\mathrm{w}} + \dot{Z}$	$(F)\ c_{\mathrm{ref,in}} = c_{\mathrm{ref,out}}$
MIX	$\dot{C}_{\mathrm{dif,dc}} + \dot{C}_{\mathrm{out}} = \dot{C}_{\mathrm{hot,in}} + \dot{C}_{\mathrm{cold,in}} + \dot{Z}$	$(F)\ c_{\mathrm{out}} = \frac{\dot{E}_{\mathrm{hot,in}} c_{\mathrm{hot,in}} + \dot{E}_{\mathrm{cold,in}} c_{\mathrm{cold,in}}}{\dot{E}_{\mathrm{hot,in}} + \dot{E}_{\mathrm{cold,in}}}$
VAL	$\dot{C}_{\mathrm{dif,dc}} + \dot{C}_{\mathrm{out}} = \dot{C}_{\mathrm{in}} + \dot{Z}$	$(F)\ c_{\mathrm{in}} = c_{\mathrm{out}}$

https://doi.org/10.52202/069564-0015

Table 8: Cost flow rates for the overall system.

System	$\dot{C}_F$	$\dot{C}_{P,CO2}$	$\dot{C}_{P,DH}$
Baseline	$\sum \dot{C}_w + \sum \dot{C}_{COOL,in}$	$\dot{C}_{CO2,out} + \sum \dot{C}_{dif,dc}$	–
DH integration	$\sum \dot{C}_w$	$\dot{C}_{CO2,out} + \frac{\dot{E}_{CO2,out} - \dot{E}_{CO2,in}}{\dot{E}_P} \sum \dot{C}_{dif,dc}$	$\dot{C}_{COOL,out} + \frac{\dot{E}_{COOL,out} - \dot{E}_{COOL,in}}{\dot{E}_P} \sum \dot{C}_{dif,dc}$

in a cooler, the fuel principle was applied to both the CO_2 stream and the DH water stream, to keep all costs in the auxiliary variable. The allocation of the total sum of $\dot{C}_{dif,dc}$ was made using the exergy value of the CO_2 product and DH as weighting factors in the absence of other valuation methods.

A set of exergoeconomic performance indicators were defined to evaluate the system. The relative cost difference (r) indicates the increase in average cost per exergy unit between fuel and product of a productive component or system, relative to the average cost of fuel supplied [22]. It is given by Eq. (10), here c_P is the average cost per unit of exergy product.

$$r = \frac{c_P - c_F}{c_F} = \frac{1-\varepsilon}{\varepsilon} + \frac{\dot{Z}}{c_F \dot{E}_P} \tag{10}$$

An exergoeconomic factor (f) was defined, as given in Eq. (11). It is the ratio between the costs coming from investment and operation to the total costs of the component or system. By using this factor, the dominating source of costs in a component can be evaluated [22]. Since costs of losses were only considered on a system level, the last term of the denominator was omitted on a component level.

$$f = \frac{\dot{Z}}{\dot{Z} + \dot{C}_D + \dot{C}_L} \tag{11}$$

3. Results

3.1. Baseline system

The baseline system had a total power consumption of 210 kW and a cooling load on the refrigeration cycle of 177 kW. Furthermore, the total cooling load in COOL1 and COOL2 was 137 kW. The total capital investment of the system was 1.7 M€. The results of the exergy and exergoeconomic analyses of the baseline system are shown in Table 9. The greatest exergy destruction was seen in the compressors and the GC, with the three highest rates of exergy destruction in COMP4 (15.1 kW), COMP1 (14.2 kW), and the GC (14.2 kW). The four compressors accounted for 56 % of the exergy destruction in the system, while the GC accounted for 14 %. Less significant contributions were found in the LIQHEX, COOL1, COOL2, VAL1, and VAL2 ranging between approx. 3 % to 8 %, while the remaining components each contributed less than 1 % to the overall exergy destruction. The results for the PUMP and the MIX were excluded from Table 9 as these components only accounted for a total of less than 0.4 % of the total exergy destruction, and less than $6 \cdot 10^{-3}$ % of the total capital investment.

The results for all material streams considered as losses are seen in Table 10. The greatest exergy losses were discharged in the GC (9.9 kW) and COOL1 (7.6 kW) accounting for 32 % and 24 % of the total losses, respectively. Losses related to cooling accounted for 85 % of the total losses in the system, while the removal of water constituted the remaining 15 %. On a system level, an exergy efficiency of 39 % was found, while 46 % of the fuel exergy being supplied was destroyed through irreversibilities in the system. The exergy losses constituted 15 % of the fuel supply on a system level.

The results of the exergy analysis indicated that the performance of the system could be improved by reducing exergy destruction, with the highest reduction potential seen in compressors and the GC and somewhat lower reduction potentials in the LIQHEX, COOL1, and COOL2. By increasing the efficiencies of compressors and decreasing the temperature difference in the LIQHEX, the exergy efficiency of the system could be directly improved. However, an improvement of the GC, COOL1, and COOL2, would reduce the destruction in these components while increasing the exergy losses. The temperature of the working media at the outlet of the components would in such case decrease and therefore a greater cooling load would be needed in the components, resulting in a greater discharge of heat to the cooling media. The analysis also showed a potential for utilising losses associated with cooling, as approx. 13 % of the fuel supply was lost in the cooling water.

Table 9: Exergy and exergoeconomic results of the baseline system. Component names refer to Fig. 2.

Component	$\dot{E}_F$ [kW]	$\dot{E}_P$ [kW]	$\dot{E}_D$ [kW]	ε [%]	γ_D [%]	$\dot{C}_F$ [€h^{-1}]	$\dot{C}_P$ [€h^{-1}]	$\dot{C}_D$ [€h^{-1}]	$\dot{Z}$ [€h^{-1}]	r [%]	f [%]
COMP1	55.9	41.7	14.2	74.6	14	4.5	12	1.1	7.24	250	86
COMP2	50.3	37.0	13.3	73.6	14	4.1	7.0	1.1	2.95	130	73
COMP3	46.1	33.1	13.0	71.8	13	3.8	4.7	1.1	0.93	74	47
COMP4	57.3	42.3	15.1	73.7	15	4.6	5.9	1.2	1.31	74	52
SEP1	264	264	0.836	99.7	0.85	11	11	0.035	0.219	2.3	86
SEP2	291	291	0.283	99.9	0.29	18	19	0.018	0.243	1.4	93
REC	162	162	0.0	100	0.0	23	23	0.0	0.0323	0.14	100
LIQHEX	328	320	8.19	97.5	8.3	23	24	0.59	0.132	3.1	18
IHEX	1.52	0.947	0.574	62.3	0.58	0.22	0.24	0.08	0.0207	76	20
COOL1	3.12	–	3.12	–	3.2	1.0	–	1.0	0.0624	–	5.9
COOL2	3.64	–	3.64	–	3.7	0.92	–	0.92	0.0245	–	2.6
COOL3	0.719	–	0.719	–	0.73	0.88	–	0.88	0.0831	–	8.7
GC	14.2	–	14.2	–	14	3.2	–	3.2	0.527	–	14
VAL1	5.77	–	5.77	–	5.9	0.82	–	0.82	0.0657	–	7.4
VAL2	3.93	–	3.93	–	4.0	0.57	–	0.57	0.0378	–	6.3
VAL3	0.894	–	0.894	–	0.91	0.13	–	0.13	0.0378	–	23
System	212	82.7	98.1	39.0	46	18	32	8.5	14.0	350	56

The results of the exergoeconomic analysis seen in Table 9 showed that the highest cost sources were the compressors and the GC, as these components had both relatively high costs associated with exergy destruction and capital investment. The CO_2 product compressors, COMP1 and COMP2, showed high relative cost differences of 250 % and 130 % meaning that the specific cost of the product stream was significantly increased compared to the fuel costs in these two components. Furthermore, COMP1 and COMP2 showed exergoeconomic factors of 86 % and 73 %, respectively, indicating that the highest cost sources in these components were capital investment. The relative cost increase in COMP3 and COMP4 of 74 % were less significant. The costs of irreversibilities and capital investment in these two components were well balanced with exergoeconomic factors of 47 % and 52 %, respectively. Looking at the heat exchangers in the system, these were generally dominated by costs associated with exergy destruction, with the greatest contributions in the GC, COOL1, COOL2, and COOL3 showing exergoeconomic factors ranging between 2 % to 14 %. At a system level, the cost rate of the product was 32 €h^{-1}, corresponding to 18.3 €t^{-1} CO_2 at the liquid product mass flow rate of 1.77 th^{-1}. The exergoeconomic factor of the overall system was 56 % indicating, that the costs associated with capital investment and inefficiencies were balanced.

The exergoeconomic analysis showed that the components in which fuel was supplied to the system were of most importance for the overall costs. The analysis indicated that the overall product cost could be reduced if the costs associated with the CO_2 product stream compressors, COMP1 and COMP2, were decreased. The

Table 10: Results for losses of the baseline system. Component names refer to Fig. 2.

Component source	$\dot{E}_L$ [kW]	γ_L [%]	$\dot{C}_L$ [€h^{-1}]
SEP1	4.1	13	0.35
SEP2	0.7	2.3	0.062
COOL1	7.6	24	0.66
COOL2	5.2	17	0.45
COOL3	3.6	12	0.31
GC	9.9	32	0.85
System	31	15	2.7

https://doi.org/10.52202/069564-0015

greatest cost contribution in these components was the capital investment, therefore, this could be decreased to potentially reduce the costs of the overall product. The external coolers showed moderate cost contributions stemming from inefficiencies. However, a reduction in exergy destruction and thereby costs associated with inefficiencies would result in increased costs of exergy losses. An alternative way of reducing the costs of inefficiencies in the external coolers could be to reduce the average cost of fuel supply to the components. This could be done if the costs of the available cooling media could be reduced.

3.2. Integration of district heat

Based on the results of the exergy and exergoeconomic analyses, it was chosen to implement DH in the external coolers to utilise the exergy loss associated with cooling and to eliminate the costs of the cooling water. The effects on the overall system costs were evaluated when DH was integrated in all coolers (COOL1, COOL2, COOL3, and the GC) and when it was only integrated in the intercoolers (COOL1, COOL2, and COOL3).

The results of the exergy and exergoeconomic analyses for the overall systems are presented in Table 11. It is seen, that the overall exergy product was increased for both DH integration options compared to the baseline system because the heating of water was now considered a product for the overall system. Therefore, the total losses were reduced to 5.0 kW and 16 kW when implementing DH in all external coolers and only in intercoolers, respectively. As a consequence, also the exergy efficiency increased for both integration options, with the highest exergy efficiency seen for the system with DH integration in all coolers because this option also utilised the heat discharged in the GC. The cooling was provided at a higher temperature with DH water. Therefore, an increase in exergy destruction was seen for both integration options which was primarily caused by increased exergy destruction in compressors and in the LIQHEX, because the temperatures at the component inlets increased. A significantly higher total exergy destruction was seen for the integration of DH in all coolers. This was caused by an increase in the optimal high pressure in the refrigeration cycle when the GC should use DH water for cooling (see Section 2.1). This significantly increased the load on COMP4, and also increased the throttling losses in VAL1.

Considering the overall system costs in Table 11, it was seen that the costs of the total system increased 11 % to 36 €h^{-1}, when DH was integrated in all coolers. This was caused by the increase of the high pressure in the refrigeration cycle, resulting in higher electricity consumption in compressors. This was also seen from the higher cost of exergy fuel of 22 €h^{-1}. The costs of the total system remained constant when DH was only implemented in intercoolers. In this integration option, the costs associated with cooling water were eliminated and outweighed the increased power consumption of compressors, meaning that the overall fuel costs remained closed to constant. The increased temperature at the suction line of COMP2 and COMP4 increased the volume flow rates, which led to greater component sizes and increased capital investment. This resulted in a cost rate of capital investment of 14.3 €h^{-1} when DH was integrated in intercoolers. For the alternative option, the capital investment showed an overall small decrease to 13.9 €h^{-1} which was caused by the GC being significantly smaller when water was used as cooling media.

When considering the costs assigned to the liquefaction and purification of CO_2, it was reduced for both implementation options. For the system with DH integration in all coolers, the CO_2 product cost was found to be $\dot{C}_{P,CO2}$ = 31.1 €h^{-1}, while it was $\dot{C}_{P,CO2}$ = 30.9 €h^{-1} when only integrating DH in existing water coolers. These costs corresponded to a specific cost of liquefaction and purification of 17.6 €t^{-1} CO_2 and 17.5 €t^{-1} CO_2, respectively. The remaining costs were assigned to the DH product. The total DH production was 168 kW at 10.1 €MWh^{-1} and 160 kW at 9.2 €MWh^{-1} when implementing DH in all coolers and only in intercoolers, respectively.

The results showed that integration of DH in the existing water coolers could be made without increasing the costs of the overall system, when assuming that the DH operators would pay for additional components needed to operate the DH. The increase in available cooling temperature increased the power consumption and the required size of the subsequent compressors, which increased the costs associated with these components. However, the costs associated with cooling were reduced, thereby reducing the costs stemming from ineffi-

Table 11: Exergy and exergoeconomic results for systems with DH integration.

DH integration	$\dot{E}_F$ [kW]	$\dot{E}_P$ [kW]	$\dot{E}_D$ [kW]	ε [%]	γ_D [%]	$\dot{C}_F$ [€h^{-1}]	$\dot{C}_P$ [€h^{-1}]	$\dot{C}_D$ [€h^{-1}]	$\dot{Z}$ [€h^{-1}]	r [%]	f [%]
COOLs and GC	272	137	130	50.2	48	22	36	11	13.9	220	56
COOLS only	224	101	107	45.2	48	18	32	8.6	14.3	300	59

ciencies in the system. The results also showed that integration of DH in the GC increased the overall system costs, due to an increased load on the high-pressure compressor. Therefore, this integration option would only be more feasible than the baseline system, if the revenue from DH sales was greater than the additional costs of the electricity consumption.

4. Discussion

The definitions of product and fuel for all components were chosen as total exergy streams. In some components and on the system level it would be more correct to divide the streams of exergy into thermal, mechanical, and chemical parts. As an example, the correct product definition of the CO_2 liquefaction and purification would be the sum of the thermal exergy in the liquid outlet stream and the increase in mechanical and chemical exergy from inlet to outlet, while the thermal exergy in the gaseous inlet stream should be considered as a fuel. This would give a negligible increase in the overall exergy product rate to 85 kW and the exergy efficiency to 39.7 %. It would result in a slightly lower product cost rate, as the costs of fuel and capital investment would not be affected by a split in exergy streams. Furthermore, it would affect the systems with DH integration in a similar way. The higher level of detail would significantly increase the computational effort of the model, and would not affect the overall conclusions of the study.

The cost balances for the external coolers were the same for both the baseline system and the systems with DH integration, even though a useful exergy product could be defined with DH integration. This approach allowed for allocation of the cooler costs between the liquefaction and purification of CO_2 and the DH production. Alternatively, all costs could be assigned to the DH product in each cooler. This would not affect the overall costs of the system, but reduce the costs assigned to the liquefaction and purification of CO_2. Furthermore, alternative methods for allocation of the costs could be used, which could distribute the costs of coolers and dissipative components in a different way between the DH product and the CO_2 product.

In both systems with DH integration, it was expected that the DH can generate positive revenue. DH integration in intercoolers would make the system more economically feasible than the baseline system, while the revenue from DH should at least exceed the additional expenses when implementing DH in all coolers. The additional costs of this system corresponded to a minimum selling price of DH of 21 €MWh^{-1}. In 2022, around 100 of the Danish DH networks had heat prices higher than 21 €MWh^{-1} [31], assuming that the heat price constituted 25 % of the price paid by consumers [32]. This indicated that the feasibility of integrating DH in all coolers depends on the local DH network. To make the conclusions on DH integration more robust, a sensitivity analysis of the ambient temperature and the yearly operating hours of the plant could be made.

The analysis also showed that the compressors were a major cost source. If the components of the systems should be changed, these should be of focus. In the systems with DH integration, it could also be beneficial to improve the performance of the coolers, as these showed moderate costs associated with inefficiencies. This would increase DH production and revenue. It would also result in a reduction of the exogenous contribution to exergy destruction in COMP2, COMP4, and the LIQHEX because the temperature at the inlet of these components would be reduced. To investigate the interdependencies between components, it could be of interest to perform an advanced exergy analysis [33]. In the present study, it was assumed that all water was removed from the CO_2, however, the amount of water that can be removed by condensation is limited by the temperature of the available cooling water. It would be relevant to also consider this influence when evaluating the effect of DH integration.

5. Conclusion

An exergoeconomic analysis of a system for liquefaction and purification of CO_2 was made. The system consisted of two-stage compression with intercooling and an external two-stage refrigeration cycle used for liquefaction. The analysis showed an exergy efficiency of 39 %, while 15 % of the supplied exergy fuel was considered as losses with the dominating part associated with external cooling. The compressors throughout the system were responsible for 56 % of the total exergy destruction and were found to be the most significant for costs. The analysis suggested that the capital investment of the two-stage compressors in the CO_2 product stream should be reduced to reduce the costs of the overall process.

It was found that integration of DH could increase the exergy efficiency to 45 % and 50 % and that the highest efficiency was achieved when all external coolers were used for DH production. However, it was seen that implementation of DH in the gascooler of the refrigeration cycle resulted in an 11 % increase in the total system costs, while DH could be integrated only in the water coolers without affecting the total costs of the system. Integration of DH increased the costs associated with compressors but reduced the costs of cooling. The analysis of the initial system also suggested that the performance of the coolers should be improved, which was expected to have a positive impact on the overall system only if DH was integrated. The study showed, that production of DH from the waste heat of the liquefaction and purification process could potentially have a positive economic impact on the system and that this was depending on the choice of integration.

https://doi.org/10.52202/069564-0015

Nomenclature

Roman Letters

$\dot{C}$	Cost rate [€s^{-1}]
$\dot{E}$	Exergy flow rate [kW]
$\dot{m}$	Mass flow rate [kgs^{-1}]
$\dot{Q}$	Heat transfer rate [kW]
$\dot{V}$	Volumetric flow rate [m^{3}s^{-1}]
$\dot{W}$	Power [kW]
$\dot{Z}$	Cost rate of owning component [€s^{-1}]
A	Area [m^2]
c	Average cost per exergy unit [€kJ^{-1}]
e	Specific exergy [kJkg^{-1}]
f	Exergoeconomic factor [%]
H	Annual operating hours [h]
h	Specific enthalpy [kJkg^{-1}]
i	Real interest rate [%]
L	Lifetime [y]
r	Relative cost difference [%]
s	Specific entropy [kJ(kgK)$^{-1}$]
T	Temperature [℃]
U	Overall heat transfer coefficient [kW(m^{2}K)$^{-1}$]
v	Velocity [ms^{-1}]
X	Primary design variable
y	Mass fraction [–]

Greek Letters

α	Scaling exponent [–]
η	Efficiency [%]
γ	Exergy ratio [–]
ε	Exergy efficiency [%]

Subscripts and superscripts

n	Chemical component
0	Reference state
a	air
CH	Chemical
CI	Capital investment
cross	Cross-sectional
D	Destruction
dc	Dissipative component
dif	Difference
disp	Displacement
F	Fuel
int	Intermediate
OM	Operation and maintenance
P	Product
PH	Physical
s	Isentropic
sys	Overall system
vol	Volumetric

Abbreviations

COMP	Compressor
COOL	Intercooler
DH	District heating
GC	Gascooler
IHEX	Internal heat exchanger
LIQHEX	Liquefaction heat exchanger
PEC	Purchased equipment cost [€]
REC	Receiver
SEP	Gas-liquid separator
TCI	Total capital investment [€]
VAL	Expansion valve

References

[1] Ritchie H., Roser M., *CO_2 and Greenhouse Gas Emissions 2020.* Available at: https://ourworldindata.org/greenhouse-gas-emissions [accessed 03.01.2022].

[2] International Energy Agency, *20 Years of Carbon Capture and Storage.* 2015 Nov. Available at: https://www.iea.org/reports/20-years-of-carbon-capture-and-storage.

[3] International Energy Agency, *Net Zero by 2050.* 2021 Oct. Available at: https://www.iea.org/reports/net-zero-by-2050.

[4] International Energy Agency, *About CCS, 2021.* Available at: https://www.iea.org/reports/about-ccus.

[5] Aspelund A., Mølnvik MJ., De Koeijer G., *Ship transport of CO_2: Technical solutions and analysis of costs, energy utilization, exergy efficiency and CO_2 emissions.* Chemical Engineering Research and Design 2006;84(9A):847-855.

[6] Seo Y., Huh C., Lee S., Chang D., *Comparison of CO_2 liquefaction pressures for ship-based carbon capture and storage (CCS) chain.* International Journal of Greenhouse Gas Control 2016;52:1-12.

[7] Roussanaly S., Deng H., Skaugen G., Gundersen T., *At what pressure shall CO_2 be transported by ship? An in-depth cost comparison of 7 and 15 barg shipping*. Energies 2021;14(18)5635.

[8] Deng H., Roussanaly S., Skaugen G., *Techno-economic analyses of CO_2 liquefaction: Impact of product pressure and impurities*. International Journal of Refrigeration 2019;103:301-315.

[9] Aspelund A., Jordal K., *Gas conditioning – The interface between CO_2 capture and transport.* International Journal of Greenhouse Gas Control 2007;1(3):343-354.

[10] Gong W., Remiezowicz E., Fosbøl PL., von Solms N., *Design and Analysis of Novel CO_2 Conditioning Process in Ship-Based CCS.* Energies 2022;15(16):5928.

[11] Alabdulkarem A., Hwang Y., Radermacher R., *Development of CO_2 liquefaction cycles for CO_2 sequestration.* Applied Thermal Engineering 2012;33-34(1):144-156.

[12] Øi LE., Eldrup N., Adhikari U., Bentsen MH., Badalge JL., Yang S., *Simulation and Cost Comparison of CO_2 Liquefaction.* Energy Procedia 2016;86:500-510.

[13] Seo Y., You H., Lee S., Huh C., Chang D., *Evaluation of CO_2 liquefaction processes for ship-based carbon capture and storage (CCS) in terms of life cycle cost (LCC) considering availability.* International Journal of Greenhouse Gas Control 2015;35:1-12.

[14] Chen F., Morosuk T., *Exergetic and economic evaluation of CO_2 liquefaction processes*. Energies 2021;14(21):7174.

[15] Aliyon K., Mehrpooya M., Hajinezhad A., *Comparison of different CO_2 liquefaction processes and exergoeconomic evaluation of integrated CO_2 liquefaction and absorption refrigeration system.* Energy Conversion and Management 2020;211:112752.

[16] Muhammad HA., Roh C., Cho J., Rehman Z., Sultan H., Baik YJ., Lee B., *A comprehensive thermodynamic performance assessment of CO_2 liquefaction and pressurization system using a heat pump for carbon capture and storage (CCS) process*. Energy Conversion and Management 2020;206:112489.

[17] Muhammad HA., Lee B., Cho J., Rehman Z., Choi B., Cho J., Roh C., Lee G., Imran M., Baik YJ., *Application of advanced exergy analysis for optimizing the design of carbon dioxide pressurization system.* Energy 2021;228:120580.

[18] Granryd E:, Ekroth I., Lundqvist P., Melinder Å., Palm B., Rohlin P., *Refrigerating Engineering.* Stockholm, Sweden: Royal Institute of Technology, KTH; 2011.

[19] Klein S.A., *EES: Engineering Equation Solver.* Available at: `https://fchartsoftware.com/ees/`.

[20] SWEP International, *SSP G8 Calculation Software*. Available at: `https://www.swep.net/support/ssp-calculation-software/ssp-g8/` [accessed 13.05.2022].

[21] Kelvion Holding, *Select RT*. Available at: `https://selectrt.kelvion.com/selector/system` [accessed 21.04.2022].

[22] Bejan A., Tsatsaronis G., Moran M., *Thermal Design & Optimization*. John Wiley & Sons, Inc.;1996.

[23] Lazzaretto A., Tsatsaronis G:, *SPECO: A systematic and general methodology for calculating efficiencies and costs in thermal systems*. Energy 2006;31(8-9):1257-1289.

[24] Woods DR., *Rules of Thumb in Engineering Practice*. Wiley-VCH Verlag GmbH & Co.; 2007.

[25] Garrett DE., *Chemical engineering economics*. Van Nostrand Reinhold; 1989.

[26] H. Jessen Jürgensen, *Prisliste 2022*. Available at: `https://www.hjj.dk/downloads-og-prislister/prisoverblik-prisbog-og-prisliste` [accessed 17.04.2022].

[27] Anderson Process, *Cat 2530 Pump*. Available at: `https://shop.andersonprocess.com/cat-2530-pump.html` [accessed 30.05.2022].

[28] SWEP International, *Heat exchangers range*. Available at: `https://www.heat-exchanger.eu/range/` [accessed 13.05.2022].

[29] Dansk Energi, *Elforsyningens nettariffer & priser pr. 1. januar 2021*. 2021 May.

[30] Danish Energy Agency, *Baggrundsnotat om elprisfremskrivninger i Analyseforudsætninger til Energinet 2021 (AF21).* 2021 Dec. Technical Report No.: 2021-6416.

[31] The Danish Utility Regulator, *Varmeprisstatistik Januar 2022*, Available at: `https://forsyningstilsynet.dk/tal-fakta/priser/varmepriser/priser-pr-1-januar-2022`.

[32] Gentofte Gladsaxe Fjernvarme, *Takstsammensætning 2022.* Available at: `https://gladsaxefjernvarme.dk/privat/faq/det-med-smaat/` [accessed 14.03.2023].

[33] Morosuk T., Tsatsaronis G., *Advanced exergy-based methods used to understand and improve energy-conversion systems*. Energy 2019;169:238-246.

https://doi.org/10.52202/069564-0015